Acoustic symmetry and vibrational anharmonicity of rhombohedral $Pb_5Ge_3O_{11}$ and $Pb_{4.7}Ba_{0.3}Ge_3O_{11}$

I. J. Al-Mummar
Department of Physics and Mathematics, University of Al-Mustansiriyah, Baghdad, Iraq

G. A. Saunders
School of Physics, University of Bath, Claverton Down, Bath, BA2 7AY, United Kingdom
(Received 16 January 1986)

Acoustic symmetry in crystals belonging to the rhombohedral $\bar{3}$ Laue group is discussed with special reference to the ultrasonic properties of $Pb_5Ge_3O_{11}$. In this material the acoustic symmetry axes are so close to the crystallographic axes that its elastic behavior is essentially that of a $\bar{3}m$ Laue group crystal. Ultrasonic wave velocities in single crystals of $Pb_5Ge_3O_{11}$ and $Pb_{4.7}Ba_{0.3}Ge_3O_{11}$ have been measured at room temperature as a function of hydrostatic pressure and uniaxial stress. Results have been used to obtain the second-order elastic constants and their hydrostatic pressure derivatives. By treating the materials as if they had $\bar{3}m$ Laue symmetry, the 14 third-order elastic constants describing the third-order elasticity of crystals have also been determined. To quantify the vibrational anharmonicities of the long-wavelength acoustic modes, the mode Grüneisen parameters have been computed and are found to be positive. This finding indicates that there is no significant acoustic mode softening induced by incipient ferroelectric optic-phonon—acoustic-phonon interactions in these materials at room temperature, which is substantially below that at which the soft optic mode, ferroelectric phase transition takes place.

I. INTRODUCTION

Pure and doped lead germanate crystals are interesting and useful ferroelectric, pyroelectric materials. The Curie point of $Pb_5Ge_3O_{11}$ is 177 °C;[1,2] alloying with barium reduces the Curie point into a temperature range more accessible to experimental studies and applications. Here the elastic constants of $Pb_5Ge_3O_{11}$ and $Pb_{4.7}Ba_{0.3}Ge_3O_{11}$ have been determined from measurements of ultrasonic wave velocities. For $Pb_5Ge_3O_{11}$ itself the results obtained can be compared with published data,[3,4] while the elastic constants have been measured for what is believed to be the first time in the barium-substituted material. The hydrostatic pressure derivatives of the elastic constants have also been determined. A central theme is a study of the symmetry of the elastic properties: the relationship between acoustic symmetry and elasticity is developed for rhombohedral crystals. $Pb_5Ge_3O_{11}$ belongs to the $R\bar{3}$ Laue group, crystals of which have a more complicated elastic behavior than those belonging to the higher symmetry $R\bar{3}m$ Laue group. However, the acoustic axes of symmetry have been found to be close to the crystallographic axes so that these materials behave as if they were $R\bar{3}m$ crystals so far as second-order elasticity is concerned. On the assumption that acoustic symmetry can be extended to a first approximation to the next order of elasticity, sets of third-order elastic constants (TOEC) have been determined for $Pb_5Ge_3O_{11}$ and $Pb_{4.7}Ba_{0.3}Ge_3O_{11}$. These TOEC have been obtained from measurements of the hydrostatic pressure and uniaxial stress derivatives of the velocities of numerous ultrasonic modes. The TOEC are used to determine the acoustic-mode Grüneisen parameters, knowledge of which is central to an understanding of properties, such as thermal expansion and nonlinear elasticity, which depend upon vibrational anharmonicity.

II. EXPERIMENTAL PROCEDURE

Good optical-quality large single-crystalline boules of $Pb_5Ge_3O_{11}$ and $Pb_{4.7}Ba_{0.3}Ge_3O_{11}$, grown by the Czochralski method, and with well-characterized growth defects,[5] were provided by Dr. G. R. Jones of Royal Signals and Radar Establishment, Malvern. Single-domain specimens were oriented by Laue back-reflection x-ray photography to within 0.5° of the selected crystallographic direction. Ultrasonic samples were cut in the form of rectangular parallelepipeds by a slow-speed diamond wheel and faces lapped flat and parallel to better than 10″ of arc. A pulse echo overlap system was used to measure the ultrasonic wave transit time. A piston and cylinder apparatus, using castor oil as the liquid pressure transmitting medium, was used to apply hydrostatic pressures up to about 1.8×10^8 Pa ($=1.8$ kbar), measured by a Manganin wire gauge. A screw press was used to apply uniaxial stress, through a proving ring to measure the applied force. To measure the dependence of ultrasonic wave velocity upon hydrostatic pressure and uniaxial stress, an automatic frequency-controlled gated carrier pulse superposition system capable of resolution to 1 part in 10^8 in these high-quality crystals, was employed.

III. SECOND-ORDER ELASTIC CONSTANTS AND ACOUSTIC SYMMETRY

For a specified crystallographic direction defined by direction cosines n_1,n_2,n_3, three bulk waves can be pro-

 ©1986 The American Physical Society

pagated with velocities and polarizations given by the Christoffel equations

$$(L_{ik}-\rho V^2\delta_{ik})U_{0K}=0,\quad i=1,2,3\ . \tag{1}$$

Here U_{01},U_{02},U_{03} are the direction cosines of the particle displacement vectors and the Christoffel coefficients for $\bar{3}$ Laue group symmetry are

$$\begin{aligned}
L_{11}&=n_1^2C_{11}+n_2^2C_{66}+n_3^2C_{44}+2n_2n_3C_{14}\ ,\\
L_{12}&=2n_1n_3C_{14}+n_1n_2(C_{11}-C_{66})\ ,\\
L_{13}&=2n_1n_2C_{14}+n_3n_1(C_{13}+C_{44})\ ,\\
L_{22}&=n_1^2C_{66}+n_2^2C_{11}+n_3^2C_{44}-2n_2n_3C_{14}\ ,\\
L_{23}&=(n_1^2-n_2^2)C_{14}+n_2n_3(C_{13}+C_{44})\ ,\\
L_{33}&=n_1^2C_{44}+n_2^2C_{44}+n_3^2C_{33}\ .
\end{aligned} \tag{2}$$

TABLE I. Mode equations and the ultrasonic wave velocities measured at 291 K.

Mode	Propagation direction N	Polarization direction U	Velocity	Relationship ($\rho V_i^2=C_{IJ}$) between velocity and elastic constants	Measured velocity (10^3 m s^{-1}) $Pb_5Ge_3O_{11}$	Measured velocity (10^3 m s^{-1}) $Pb_{4.7}Ba_{0.3}Ge_3O_{11}$
Pure longitudinal	[100]	[100]	V_1	C_{11}	3.029	3.033
Pure shear	[100]		V_2	$\frac{1}{2}\{(C_{66}+C_{44})+[(C_{44}-C_{66})^2+4C_{14}^2]^{1/2}\}$	1.706	1.706
Pure shear	[100]		V_3	$\frac{1}{2}\{(C_{66}+C_{44})-[(C_{44}-C_{66})^2+4C_{14}^2]^{1/2}\}$	1.671	1.696
Pure longitudinal	[010]	[010]	V_4	$\frac{1}{2}\{(C_{11}+C_{44})+[(C_{44}-C_{11})^2+4C_{14}^2]^{1/2}\}$	3.086	2.988
Pure shear	[010]	[100]	V_5	$C_{66}=\frac{1}{2}(C_{11}-C_{12})$	1.702	1.696
Quasi shear	[010]	[001]	V_6	$\frac{1}{2}\{(C_{11}+C_{44})-[(C_{44}-C_{11})^2+4C_{14}^2]^{1/2}\}$	1.724	1.698
Pure longitudinal	[001]	[001]	V_7	C_{33}	3.570	3.432
Pure degenerate shear	[001]		V_8	C_{44}	1.723	1.723
Quasi longitudinal	$\left[0\frac{1}{\sqrt{2}}\frac{1}{\sqrt{2}}\right]$		V_9	$\frac{1}{2}(\frac{1}{2}(C_{11}+C_{33})+C_{44}-C_{14}+\{[\frac{1}{2}(C_{11}-C_{33})-C_{14}]^2+(C_{13}+C_{44}-C_{14})^2\}^{1/2})$	3.080	3.095
Pure shear	$\left[0\frac{1}{\sqrt{2}}\frac{1}{\sqrt{2}}\right]$	[100]	V_{10}	$\frac{1}{2}(C_{66}+C_{44})+C_{14}$	1.725	1.695
Quasi shear	$\left[0\frac{1}{\sqrt{2}}\frac{1}{\sqrt{2}}\right]$		V_{11}	$\frac{1}{2}(\frac{1}{2}(C_{11}+C_{33})+C_{44}-C_{14}-\{[\frac{1}{2}(C_{11}-C_{33})-C_{14}]^2+(C_{13}+C_{44}-C_{14})^2\}^{1/2})$	2.035	1.998
Quasi longitudinal	$\left[0-\frac{1}{\sqrt{2}}\frac{1}{\sqrt{2}}\right]$		V_{12}	$\frac{1}{2}(\frac{1}{2}(C_{11}+C_{33})+C_{44}+C_{14}+\{[\frac{1}{2}(C_{11}-C_{33})+C_{14}]^2+(C_{13}+C_{44}+C_{14})^2\}^{1/2})$	3.136	3.065
Pure shear	$\left[0-\frac{1}{\sqrt{2}}\frac{1}{\sqrt{2}}\right]$	[100]	V_{13}	$\frac{1}{2}(C_{66}+C_{44})-C_{14}$	1.695	1.707
Quasi shear	$\left[0-\frac{1}{\sqrt{2}}\frac{1}{\sqrt{2}}\right]$		V_{14}	$\frac{1}{2}(\frac{1}{2}(C_{11}+C_{33})+C_{44}+C_{14}-\{[\frac{1}{2}(C_{11}-C_{33})+C_{14}]^2+(C_{13}+C_{44}+C_{14})^2\}^{1/2})$	2.034	2.009

The elastic stiffness constant matrix in the crystallographic axis (X,Y,Z) reference frame for a $\bar{3}$ crystal is

$$\begin{bmatrix} C_{11} & C_{12} & C_{13} & C_{14} & -C_{25} & 0 \\ C_{12} & C_{11} & C_{13} & -C_{14} & C_{25} & 0 \\ C_{13} & C_{13} & C_{33} & 0 & 0 & 0 \\ C_{14} & -C_{14} & 0 & C_{44} & 0 & -C_{25} \\ -C_{25} & C_{25} & 0 & 0 & C_{44} & C_{14} \\ 0 & 0 & 0 & C_{25} & C_{14} & C_{66} \end{bmatrix}, \quad (3)$$

where $C_{66}=\frac{1}{2}(C_{11}-C_{12})$. Measurements were made on [100], [010], [0 $1/\sqrt{2}$ $1/\sqrt{2}$], and [0 $-1/\sqrt{2}$ $1/\sqrt{2}$] samples; solutions of the equation of motion for these propagation directions, together with the ultrasonic wave velocities measured at room temperature (291 K), are given in Table I. Setting up the ultrasonic experiments requires knowledge of the polarization vectors. For the quasishear and quasilongitudinal modes propagated in the [010] direction the particle displacement vector makes an angle θ with the XY plane given by

$$\tan\theta=U_{03}/U_{02}=C_{14}/(C_{11}-\rho V_{4,6}^2) \quad (4)$$

which is accidentally zero for both lead germanate and barium-doped lead germanate. For the two pure-shear waves which can be propagated in the [100] direction, the particle displacement vector makes an angle ϕ with the XY plane given by

$$\tan\phi=-[C_{14}/(C_{44}-\rho V_{2,3}^2)] \quad (5)$$

and is again accidently zero. For propagation in the [0 $-1/\sqrt{2}$ $1/\sqrt{2}$] direction, the particle displacement vector makes an angle of δ with the XY plane for the quasilongitudinal mode where

$$\tan\delta=\pm(C_{14}+\tfrac{1}{2}C_{11}+\tfrac{1}{2}C_{44} -\rho V_{12}^2)/\tfrac{1}{2}(C_{13}+C_{44}+C_{14}) . \quad (6)$$

For the quasishear mode of velocity V_{14}, the corresponding angle is $\delta+\pi/2$. For $Pb_5Ge_3O_{11}$ and $Pb_{4.7}Ba_{0.3}Ge_3O_{11}$ δ has been calculated as 54°31′ and 51°53′, respectively. The densities of both $Pb_5Ge_3O_{11}$ and $Pb_{4.7}Ba_{0.3}Ge_3O_{11}$ were measured by Archimedes' principle as 7390 kg m^{-3}. The second-order adiabatic elastic stiffness constants (SOEC) of $Pb_5Ge_3O_{11}$, compared with values reported previously, and of $Pb_{4.7}Ba_{0.3}Ge_3O_{11}$ are given in Table II. The uncertainties arising from mode consistencies, errors in density and ultrasonic path length measurements, and the small piezoelectric correction amount to about 1%. For the compound itself the SOEC obtained are nearly identical to the earlier data.[3,4] The components of the adiabatic elastic compliances are shown in Table III.

If an ultrasonic wave is propagated through a crystal, the symmetry of the system includes an inversion center because it does not matter in which direction the wave travels. Hence it is the Laue group which is relevant to elasticity theory. Furthermore, for certain crystal systems the minimum number of invariants required to detail the elastic behavior need not—in a restricted sense—be the

TABLE II. Adiabatic SOEC of $Pb_5Ge_3O_{11}$ and $Pb_{4.7}Ba_{0.3}Ge_3O_{11}$ at room temperature (291 K). (Units are 10^{10} N m^{-2}.)

	$Pb_5Ge_3O_{11}$			$Pb_{4.7}Ba_{0.3}Ge_3O_{11}$
C_{IJ}	a	Ref. 4	Ref. 3	a
C_{11}	6.78	6.80	6.84	6.8
C_{12}	2.50	2.57	2.68	2.54
C_{13}	1.79	1.89	1.79	1.93
C_{14}	0.004	0.00	0.00	0.00
C_{25}	0.00	0.00	0.12	0.00
C_{33}	9.42	9.42	9.43	8.70
C_{44}	2.20	2.23	2.26	2.20
C_{66}	2.14	2.11	2.08	2.13

[a]Present work.

elastic stiffnesses C_{ijkl} referred to the conventional crystallographic coordinate axes as a basis. By a suitable choice of coordinates, including pure mode axes which in themselves are not crystal symmetry axes, the number of invariant components of the elastic stiffness tensor can be reduced.[6,7] Thus, using an orthogonal basis of vectors $\mathbf{e}_a$ $(a=0,+1,-1)$ on which the second-order elastic stiffness tensor components are referred to as $C_{\mu\nu\sigma\tau}(a,b,c,d=0,+1,-1)$ and transform as

$$C'_{abcd}=e^{-i(a+b+c+d)\phi}C_{abcd} \quad (7)$$

it can be shown that if $\mathbf{e}_0$ is directed along the major symmetry axis L^n, the tensor components $C_{\mu\nu\sigma\tau}$ become zero when

$$e^{i(a+b+c+d)(2\pi/n)}\neq 1 . \quad (8)$$

The angle ϕ is a rotation about the L^n axis (the threefold axis in a $\bar{3}$ rhombohedral crystal).

Such a transformation with a basis vector (Z) along a threefold axis for a $\bar{3}$ rhombohedral crystal gives

$$\begin{aligned} &C'_{14}=-C'_{24}=C'_{56}=C_{14}\cos(3\phi)+C_{25}\sin(3\phi) , \\ &C'_{25}=C'_{15}=C'_{46}=-C_{14}\sin(3\phi)+C_{25}\cos(3\phi) , \\ &C'_{33}=C_{33},\ C'_{44}=C_{44}=C_{55} , \\ &C'_{13}=C_{13}=C'_{23} , \\ &C'_{34}=C_{35}=C'_{45}=C'_{36}=0 . \end{aligned} \quad (9)$$

TABLE III. Adiabatic elastic compliances of $Pb_5Ge_3O_{11}$ and $Pb_{4.7}Ba_{0.3}Ge_3O_{11}$ at 291 K (units are 10^{-10} N^{-1} m^2).

	$Pb_5Ge_3O_{11}$		$Pb_{4.7}Ba_{0.3}Ge_3O_{11}$
S_{IJ}	a	Ref. 3	a
S_{11}	0.175	0.177	0.176
S_{12}	−0.059	−0.064	−0.059
S_{13}	−0.023	−0.022	−0.026
S_{14}	0.00	0.00	0.00
S_{25}	0.00	0.00	0.00
S_{33}	0.115	0.114	0.125
S_{44}	0.455	0.445	0.455
S_{66}	0.47	0.483	0.47

[a]Present work.

The rotation ϕ transforms from the crystallographic axes X and Y to pure mode axes X' and Y'. The elastic stiffness tensor components C_{11}, C_{33}, C_{44}, C_{12}, C_{66}, and C_{13} are invariant for this rotation. When the transformation angle takes the particular value ϕ_A given by

$$\phi_A = \tfrac{1}{3}\tan^{-1}\left[\frac{C_{25}}{C_{14}}\right] \tag{10}$$

then C'_{25} becomes zero. The axial direction X' at the angle ϕ_A is a pure mode axis, referred to as an acoustic symmetry axis.[8] The elastic stiffness matrix C'_{IJ} referred to the transformed axial set X',Y',Z (Y' completes the orthogonal axial set) then takes the form for that of the $\bar{3}m$ rhombohedral Laue group crystals

$$\begin{vmatrix} C_{11} & C_{12} & C_{13} & C_{14} & 0 & 0 \\ C_{12} & C_{11} & C_{13} & -C_{14} & 0 & 0 \\ C_{13} & C_{13} & C_{33} & 0 & 0 & 0 \\ C_{14} & -C_{14} & 0 & C_{44} & 0 & 0 \\ 0 & 0 & 0 & 0 & C_{44} & C_{14} \\ 0 & 0 & 0 & 0 & C_{14} & C_{66} \end{vmatrix} . \tag{11}$$

Therefore, in this frame of reference the symmetry of the elastic properties of $\bar{3}$ Laue group crystals is the same as that of $\bar{3}m$ Laue group crystals. Then the number of independent elastic constants is reduced from seven (C_{IJ}) to six (C'_{IJ}); the angle ϕ_A made by the acoustic symmetry axis X' with the crystallographic axis X is another unknown, and can be determined from Eqs. (9) once the elastic constants have been measured. In $\bar{3}m$ crystals the presence of vertical planes of symmetry and/or dyad axes in the Z planes requires that C_{25} (or S_{25}) be zero: the pure mode axes coincide with the crystallographic axes and there are only six independent elastic stiffness components. Three acoustic symmetry axes exist in the Z plane because Eq. (10) has three equal roots separated by $\pi/3$ in a 2π cycle (or six if it is recalled that there is an inversion center added for propagation of a lattice vibration so that mode velocity is the same in the X' and $-X'$ directions). The acoustic symmetry axes are so-called because the elastic properties referred to them as a basis exhibit the same acoustic symmetry properties as those in the higher-symmetry Laue group.[8] The elastic properties are symmetrical with respect to acoustic mirror planes normal to the acoustic symmetry axes.

The measurements of the elastic stiffness tensor components of $Pb_5Ge_3O_{11}$ and $Pb_{4.7}Ba_{0.3}Ge_3O_{11}$ (Table II) enable determination of the positions of the acoustic symmetry axes in these crystals. In fact the observation that C_{25} is so close to zero shows that for both materials the acoustic symmetry axes lie within experimental error along the Y axis (and also in the two threehold rotation-symmetry-related directions at $\pm 120°$ to the Y axis in the Z plane). In general, reference of the elastic properties to the acoustic symmetry axes as a basis affords a useful simplification for crystals belonging to the $\bar{3}$ Laue group; in the case of $Pb_5Ge_3O_{11}$ and $Pb_{4.7}Ba_{0.3}Ge_3O_{11}$ the elastic behavior already corresponds very closely to that of a $\bar{3}m$ Laue group crystal. Actually a further simplification is also possible. Since C_{14} is also effectively zero within experimental error, the two materials of this study could be treated elastically as if they were hexagonal crystals belonging to the *HI* Laue group having only five invariant parameters: C_{11}, C_{13}, C_{33}, C_{44}, and C_{66}.

Knowledge of the complete set of elastic stiffness tensor components permits determination of a material's response to a moderate applied stress system. Particularly useful in relating theoretically the interatomic binding forces and elasticity are the linear (β_{XY} and β_Z) and volume (β_V) compressibilities

$$\beta_{XY} = S_{11} + S_{12} + S_{13} , \tag{12}$$

$$\beta_Z = 2S_{13} + S_{33} , \tag{13}$$

$$\beta_V = 2S_{11} + S_{33} + 4S_{13} + 2S_{12} , \tag{14}$$

which (in units of 10^{-12} m^2N^{-1}) are 9.3, 6.95, and 25.5, respectively, for $Pb_5Ge_3O_{11}$ and 9.1, 7.3, and 25.5, respectively, for $Pb_{4.7}Ba_{0.3}Ge_3O_{11}$. Thus barium-doped lead germanate is rather more compressible along the trigonal direction than $Pb_5Ge_3O_{11}$. The bulk moduli ($1/\beta_V$) of both materials are 3.9×10^{10} $N\,m^{-2}$.

IV. HYDROSTATIC PRESSURE DERIVATIVES OF THE ELASTIC CONSTANTS

The ultrasonic wave transit times have been measured as a function of hydrostatic pressure using a pulse superposition technique[9] which leads to the gradient f' of the measured superposition frequency f as a function of pressure. To bypass the need to calculate directly the changes

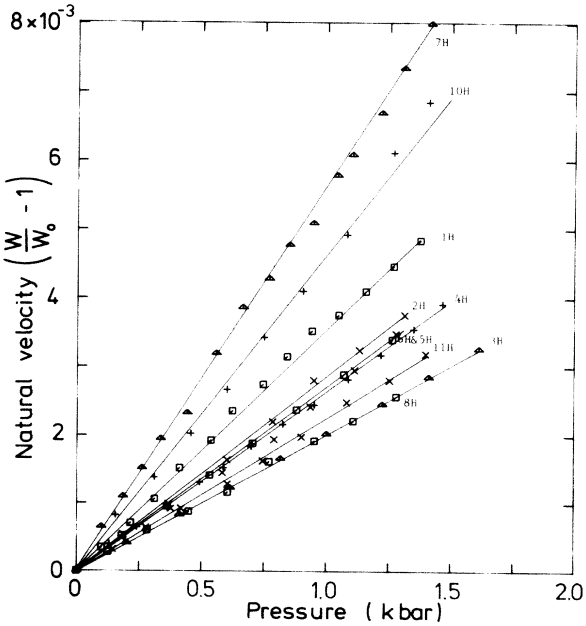

FIG. 1. Relative changes induced by hydrostatic pressure on the natural wave velocities of ultrasonic modes propagated in $Pb_5Ge_3O_{11}$. The modal configurations and values of $(\rho_0 W^2)'_{P=0}$ derived from these data are listed in Table IV.

TABLE IV. Mode equations and measured values of $(\rho_0 W^2)'_{P=0}$ under hydrostatic pressure.

Mode	Propagation direction	Polarization direction	F_H	G_H	$Pb_5Ge_3O_{11}$	$Pb_{4.7}Ba_{0.3}Ge_3O_{11}$
$1H$	[100]	[100]	S_1	$S_1(C_{111}+C_{112})+S_3C_{113}$	4.858	3.87
$2H$	[100]	[010]	$S_1\beta_1^2+S_3\alpha_1^2$	$\frac{1}{2}S_1(C_{222}-C_{112})+S_3(C_{113}-C_{123})$	1.003	1.3
$3H$	[100]	[001]	$S_1\alpha_1^2+S_3\beta_1^2$	$S_1(C_{155}+C_{144})+S_3C_{344}$	1.218	1.19
$4H$	[010]	[010]	$S_1\alpha_2^2+S_3\beta_2^2$	$S_1(C_{112}+C_{111})+S_3C_{113}$	3.68	3.98
$5H$	[010]	[100]	$S_1\beta_2^2+S_3\alpha_2^2$	$\frac{1}{2}S_1(C_{222}-C_{112})+\frac{1}{2}S_3(C_{113}-C_{123})$	1.22	1.20
$6H$	[010]	[001]	S_1	$S_1(C_{144}+C_{155})+S_3C_{344}$	1.18	1.27
$7H$	[001]	[001]	S_3	$2S_1C_{133}+S_3C_{333}$	10.46	10.47
$8H$	[001]	[100] or [010]	S_1	$S_1(C_{144}+C_{155})+S_3C_{344}$	0.88	1.27
$10H$	$\left[0\ \frac{1}{\sqrt{2}}\ \frac{1}{\sqrt{2}}\right]$	$\left[0\ \frac{1}{\sqrt{2}}\ \frac{1}{\sqrt{2}}\right]$	$S_1\alpha_3^2+S_3\beta_3^2$	$\frac{1}{4}S_1(C_{111}+C_{112}+4C_{144}+2C_{123}+4C_{114}-4C_{124}+4C_{155}+2C_{113}+2C_{133})+\frac{1}{4}S_3(C_{113}+2C_{133}-4C_{134}+4C_{344}+C_{333})$	6.76	7.37
$11H$	$\left[0\ \frac{1}{\sqrt{2}}\ \frac{1}{\sqrt{2}}\right]$	$\left[0-\frac{1}{\sqrt{2}}\ \frac{1}{\sqrt{2}}\right]$	$S_1\beta_3^2+S_3\alpha_3^2$	$\frac{1}{4}S_1(C_{111}+C_{112}-2C_{123}+C_{133})+\frac{1}{4}S_3C_{333}+\frac{1}{4}C_{133}(S_{11}+S_{12}-3S_{13}-2S_{33})+\frac{1}{2}C_{113}(-2S_{11}-2S_{12}+S_{33})$	1.19	1.17

$[S_1=(S_{11}+S_{12}+S_{13})$ and $S_3=(S_{33}+2S_{13}]$

α_i is the cosine and β_i is the sine of these angles θ, ϕ, or δ.

$\alpha_1=1,{}^a\alpha_2=1,{}^b\ \alpha_3=0.583^c$

$\beta_1=0,{}^a\beta_2=0,{}^b\beta_3=0.815^c$

[a] $\tan\theta=0$ [Eq. (4)]. [b] $\tan\phi=0$ [Eq. (5)]; for $Pb_5Ge_3O_{11}$ and $Pb_{4.7}Ba_{0.3}Ge_3O_{11}$.

[c] $\tan\delta=1.397$ [Eq. (6)] for $Pb_5Ge_3O_{11}$ and $\tan\phi=1.26$ for $Pb_{4.7}Ba_{0.3}Ge_3O_{11}$.

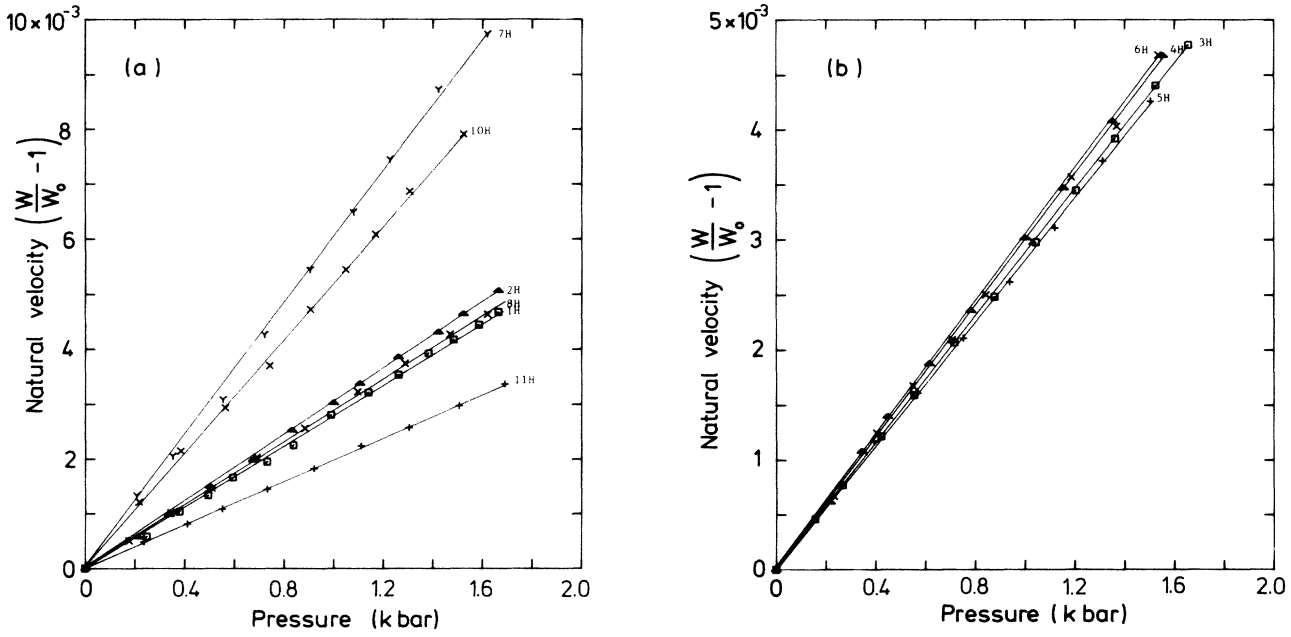

FIG. 2. Relative changes induced by hydrostatic pressure on the natural wave velocities of ultrasonic modes propagated in $Pb_{4.7}Ba_{0.3}Ge_3O_{11}$. The modal configurations and values of $(\rho_0 W^2)'_{P=0}$ derived from these data are listed in Table IV.

in crystal dimensions induced by the application of pressure, the "natural velocity" W technique[10] has been used. The effects of hydrostatic pressure on the natural velocity are shown in Fig. 1 for $Pb_5Ge_3O_{11}$ and in Fig. 2 for $Pb_{4.7}Ba_{0.3}Ge_3O_{11}$. The hydrostatic pressure derivatives $(\rho_0 W^2)'_{P=0}$ obtained from these measurements are collected in Table IV. The hydrostatic pressure derivatives $(\partial C_{IJ}/\partial P)_{P=0}$ were obtained using[11]

$$
\begin{aligned}
&\partial C_{11}/\partial P = C_{11}[(2f'/f_0)+2S_{13}+S_{33}], \quad \mathbf{N}\|[100], \ \mathbf{U}\|[100] \\
&\partial C_{66}/\partial P = C_{66}[(2f'/f_0)+2S_{13}+S_{33}], \quad \mathbf{N}\|[010], \ \mathbf{U}\|[100] \\
&\partial C_{33}/\partial P = C_{33}[(2f'/f_0)+2S_{11}+2S_{13}-S_{33}], \quad \mathbf{N}\|[001], \ \mathbf{U}\|[001] \\
&\partial C_{44}/\partial P = C_{44}[(2f'/f_0)+2S_{11}+2S_{12}-S_{33}], \quad \mathbf{N}\|[001], \ \mathbf{U}\perp[001] \\
&\partial C'/\partial P = C'[(2f'/f_0)+S_{11}+S_{12}+S_{13}] \ \text{(see Table I)}, \\
&\partial C''/\partial P = C''[(2f'/f_0)+2S_{13}+S_{33}] \ \text{(see Table I)},
\end{aligned}
\tag{15}
$$

where

$$C' = \tfrac{1}{2}\{(C_{11}+C_{33})/2+C_{44}-C_{14}-[(C_{11}/2-C_{33}/2-C_{14})^2+(C_{13}+C_{44}-C_{14})^2]^{1/2}\}$$

TABLE V. Hydrostatic pressure derivatives of effective $(\partial C_{IJ}/\partial P)$ and thermodynamic (B_{IJ}) second-order elastic constants of crystals with rhombohedral structure.

	$Pb_5Ge_3O_{11}$	$Pb_{4.7}Ba_{0.3}Ge_3O_{11}$	Bi Ref. 11	Quartz Ref. 12	Calcite Ref. 13	Al_2O_3 Ref. 14
$\partial C_{11}/\partial P$	5.33	4.33	6.38	3.28	3.02	3.591
$\partial C_{12}/\partial P$	2.59	1.79	2.38	8.66	2.05	0.336
$\partial C_{13}/\partial P$	3.41	4.43	4.69	5.97	3.19	1.121
$\partial C_{14}/\partial P$	0.00	0.00	1.70	1.93	−1.25	0.211
$\partial C_{25}/\partial P$	0.0	0.0				
$\partial C_{33}/\partial P$	11.96	11.42	6.62	10.84	2.80	2.967
$\partial C_{44}/\partial P$	1.15	1.51	3.37	2.66	0.92	2.394
$\partial C_{66}/\partial P$	1.39	1.35	2.00	−2.69	0.49	1.628

and

$$C''=\tfrac{1}{2}\{(C_{66}+C_{44})+[(C_{44}-C_{66})^2+4C_{14}^2]^{1/2}\}$$

and are compared with those of other crystals having the rhombohedral structure in Table V. **N** and **U** correspond to the wave propagation and polarization directions, respectively.

The ferroelectric phase transition takes $Pb_5Ge_3O_{11}$ from the point group 3 in the ferroelectric phase to $\bar{6}$ in the paraelectric phase[3] and is driven by optic-phonon mode softening.[15,16] The elastic constants C_{11}, C_{33}, C_{12}, and C_{13} show, as a function of temperature, downward-directed cusplike anomalies in the vicinity of the Curie point, anomalies probably caused by the soft Raman active mode giving an internal strain contribution to the elastic constants.[4] The temperature-dependent reduction of the elastic stiffness is not reflected in the effects of hydrostatic pressure: each $(\partial C_{IJ}/\partial P)$ is positive, whereas a strong soft optic-mode—acoustic-mode interaction might be expected to produce negative derivatives. The finding of positive derivatives is not surprising—the pressure effects have been measured at room temperature, substantially below the Curie point for both materials.

V. THIRD-ORDER ELASTIC CONSTANTS AND ACOUSTIC-MODE GRÜNEISEN PARAMETERS

The values of $\partial C_{25}/\partial P$ and $\partial C_{14}/\partial P$ are zero within experimental error. Hence the shift of the acoustic symmetry axes with respect to the crystallographic axes is negligibly small at the comparatively low hydrostatic parameters used in the experiment; it was decided to treat $Pb_5Ge_3O_{11}$ and $Pb_{4.7}Ba_{0.3}Ge_3O_{11}$ elastically as $\bar{3}m$ Laue group crystals at third order—probably a reasonable approximation, although not so good as at second order. For it to be accurate, shifts of the acoustic symmetry axes with uniaxial stress should be small in comparison with changes produced by such a stress on the ultrasonic wave velocities. To obtain the TOEC, the velocity changes induced by uniaxial stress have been measured for 20 modes, to be employed in addition to the ten modes examined under hydrostatic pressure. The results obtained for $Pb_5Ge_3O_{11}$ are shown in Fig. 3; similar data sets have been measured for $Pb_{4.7}Ba_{0.3}Ga_3O_{11}$. To obtain sets of TOEC (Table VI), values of $(\rho_0 W^2)'_{P=0}$ obtained from these data have been combined with those obtained under hydrostatic pressure in a least-mean-squares fit to the relationships given in Tables IV and VII.

The anharmonicity of lattice vibrations is responsible for thermal expansion as well as the nonlinear behavior of a crystal under finite strain. Thermal expansion data is usually interpreted in the light of the thermal Grüneisen parameter γ^{th}, which for a uniaxial crystal has two components:

$$\gamma_{\perp}^{\text{th}}=[(C_{11}+C_{12})\alpha_{11}+C_{13}\alpha_{33}]V/C_p=+0.84$$

for $Pb_5Ge_3O_{11}$

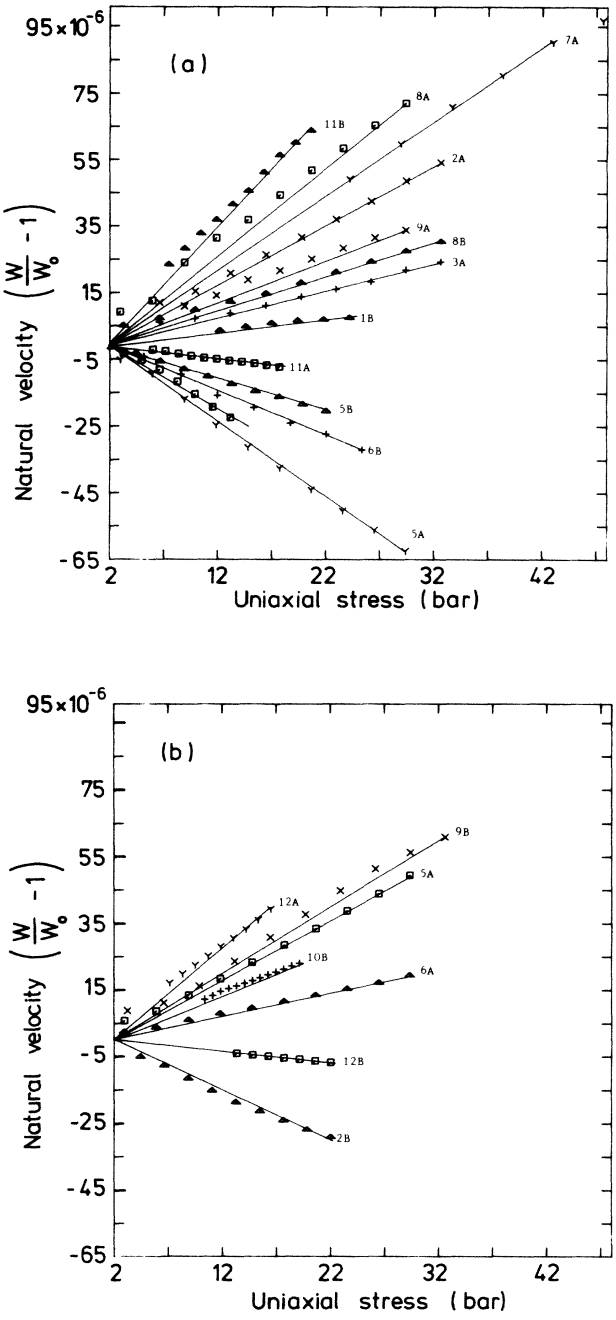

FIG. 3. Relative changes induced by uniaxial stress on the natural wave velocities of ultrasonic modes propagated in $Pb_5Ge_3O_{11}$. The modal and stress configurations are listed in Table VII.

$$\gamma_{||}^{\text{th}}=(2C_{13}\alpha_{11}+C_{33}\alpha_{33})V/C_p=+0.91$$

for $Pb_5Ge_3O_{11}$

in directions in the XY plane and Z axis, respectively. Thus the value for γ^{th} for $Pb_5Ge_3O_{11}$ is given by

$$\gamma^{\text{th}}=(2\gamma_{\perp}^{\text{th}}+\gamma_{||}^{\text{th}})/3=0.86\ . \qquad (16)$$

TABLE VI. The third-order elastic constants (in units of $10^{11}\,\mathrm{N\,m^{-2}}$) of $Pb_5Ge_3O_{11}$ and $Pb_{4.7}Ba_{0.3}Ge_3O_{11}$ treated in the $\bar{3}m$ Laue group approximation compared with those of other rhombohedral crystals.

Constant	$Pb_5Ge_3O_{11}$	$Pb_{4.7}Ba_{0.3}Ge_3O_{11}$	Bi Ref. 11	Quartz Ref. 17	Calcite Ref. 13	Al_2O_3 Ref. 14	$LiNbO_3$ Ref. 18
C_{111}	−5.06	−5.35	−7.14	−2.10	−5.79	−38.7	−5.12
C_{112}	−0.248	−0.33	1.16	−3.45	−1.47	−10.9	4.54
C_{113}	−1.69	−1.5	−1.78	0.12	−1.93	−9.63	7.28
C_{114}	0.30	0.52	−3.77	−1.63	2.18	0.55	−4.10
C_{123}	−0.81	−1.65	−1.27	−2.94	−0.41	−2.89	0.79
C_{124}	0.18	−0.31	−0.70	−0.15	−0.10	−0.39	0.55
C_{133}	−4.2	−4.98	−1.62	−3.12	−2.39	−0.22	−0.34
C_{134}	−0.54	−0.74	0.43	0.02	0.82	−1.31	−0.01
C_{144}	−0.71	−1.02	−0.50	−1.34	−0.69	−3.02	−0.37
C_{155}	−1.36	−1.5	−4.06	−2.00	−1.39	−11.6	−5.99
C_{222}	−5.5	−5.3	−5.77	−3.32	−6.75	−45.2	−5.99
C_{333}	−7.06	−4.7	−4.03	−8.15	−4.98	−32.4	−4.78
C_{344}	−0.49	−0.29	−0.95	−1.10	−1.95	−10.9	−5.40
C_{444}	−0.12	−0.37	1.77	−2.76	0.33	−0.19	−0.41

This thermodynamic parameter γ^{th} is the weighted average of mode Grüneisen parameters

$$\gamma^{\mathrm{th}}=\sum_i C_i\gamma_i \Big/ \sum C_i,\quad \gamma_i=-(\partial \ln\omega_i/\partial \ln V)\,, \qquad (17)$$

where ω_i is the frequency of mode i and C_i is the heat capacity per mode. Thus γ^{th} includes contributions from all the modes of vibration. The TOEC can be used to provide a measure of the contributions specifically from the long-wavelength acoustic modes alone.

The acoustic-mode Grüneisen parameters have been calculated as a function of propagation direction for $Pb_5Ge_3O_{11}$ and $Pb_{4.7}Ba_{0.3}Ge_3O_{11}$. The methods adopted and the necessary relationships have been detailed[11] for $\bar{3}m$ Laue group crystals and are applicable to $\bar{3}$ crystals by a transformation from crystallographic to acoustic symmetry axes (negligible in the present case). The results obtained plotted in Figs. 4 and 5 are positive for all modes—reemphasizing the absence of softening of the long-wavelength acoustic-phonon modes.

For $Pb_5Ge_3O_{11}$ the Debye temperature [=230 K (Ref.

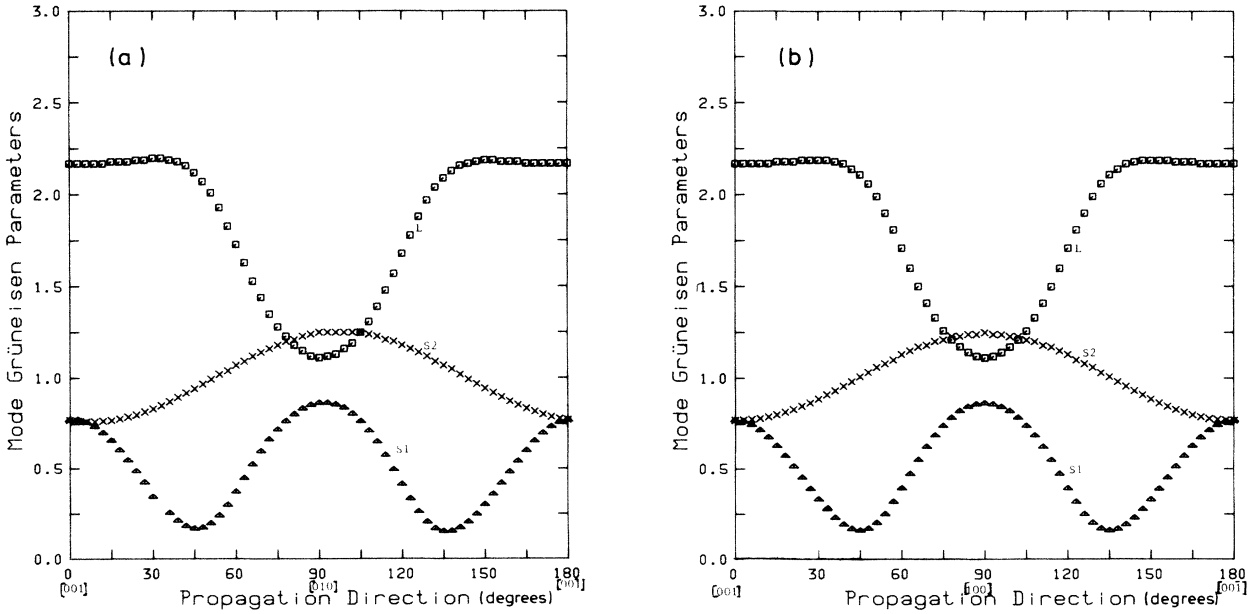

FIG. 4. The zone center acoustic-mode Grüneisen parameters as a function of propagation direction in (a) the YZ and (b) the XZ planes of $Pb_5Ge_3O_{11}$.

TABLE VII. Mode equations: expressions for F and G under uniaxial stress for $\bar{3}m$ Laue group crystals.

Mode	Propagation direction	Polarization direction	Stress direction	Case	F_U	G_U
1*A*	[100]	[100]	[010]	$M_2\gamma L$	S_{12}	$S_{12}C_{111}+S_{11}C_{112}+S_{13}C_{113}-2S_{14}C_{114}$
1*B*	[100]	[100]	[001]	$M_3\gamma L$	S_{13}	$S_{13}(C_{111}+C_{112})+S_{33}C_{113}$
2*A*	[100]	$[0\ \beta_1\ -\alpha_1]$	[010]	$M_2\gamma T'$	$\beta_1^2S_{11}+\alpha_1^2S_{13}+\alpha_1\beta_1S_{14}$	$\frac{1}{4}S_{12}(-2C_{111}-C_{112}+3C_{222})$ $+\frac{1}{4}S_{14}(2C_{111}-C_{112}+C_{222})$ $+\frac{1}{2}S_{13}(C_{113}-C_{123})-2S_{14}C_{124}$
2*B*	[100]	$[0\ \beta_1\ -\alpha_1]$	[001]	$M_3\gamma T'$	$\beta_1^2S_{13}+\alpha_1^2S_{33}$	$\frac{1}{2}S_{13}(C_{222}-C_{112})+\frac{1}{2}S_{33}(C_{113}-C_{123})$
3*A*	[100]	$[0\ \alpha_1\ \beta_1]$	[010]	$M_2\gamma T''$	$\alpha_1^2S_{11}+\beta_1^2S_{13}-\alpha_1\beta_1S_{14}$	$S_{12}C_{155}+S_{11}C_{144}+S_{13}C_{344}+2S_{14}C_{444}$
3*B*	[100]	$[0\ \alpha_1\ \beta_1]$	[001]	$M_3\gamma T''$	$\alpha_1^2S_{13}+\beta_1^2S_{33}$	$S_{13}(C_{155}+C_{144})+S_{33}C_{344}$
4*A*	[010]	$[0\ \alpha_2\ \beta_2]$	[100]	$M_1\gamma' L$	$\beta_2^2S_{13}+\alpha_2^2S_{12}+\alpha_2\beta_2S_{14}$	$S_{11}C_{144}+S_{12}C_{155}+S_{13}C_{344}+2S_{14}C_{444}$
4*B*	[010]	$[0\ \alpha_2\ \beta_2]$	[001]	$M_3\gamma' L$	$\alpha_2^2S_{13}+\beta_2^2S_{33}$	$S_{13}(C_{111}+C_{112})+S_{33}C_{113}$
5*A*	[010]	$[0\ \beta_2\ -\alpha_2]$	[100]	$M_1\gamma T'$	$\alpha_2^2S_{13}+\beta_2^2S_{12}-\alpha_2\beta_2S_{14}$	$S_{11}(C_{111}+C_{112}-C_{222})+S_{12}C_{222}$ $+S_{13}C_{113}+2S_{14}(-C_{114}-2C_{124})$
5*B*	[010]	$[0\ \beta_2\ -\alpha_2]$	[001]	$M_3\gamma T'$	$\beta_2^2S_{13}+\alpha_2^2S_{33}$	$S_{13}(C_{155}+C_{144})+S_{33}C_{344}$
6*A*	[010]	[100]	[100]	$M_1\gamma' T''$	S_{11}	$\frac{1}{4}S_{11}(-2C_{111}-C_{112}+3C_{222})$ $+\frac{1}{4}S_{12}(2C_{111}-C_{112}-C_{222})$ $+\frac{1}{2}S_{13}(C_{113}-C_{123})+2S_{14}C_{124}$
6*B*	[010]	[100]	[001]	$M_3\gamma' T''$	S_{13}	$\frac{1}{2}S_{13}(C_{222}-C_{112})+\frac{1}{2}S_{33}(C_{113}-C_{123})$
7*A*	[001]	[001]	[100]	$M_1\alpha L$	S_{13}	$(S_{11}+S_{12})C_{133}+S_{13}C_{333}$
7*B*	[001]	[001]	[010]	$M_2\alpha L$	S_{13}	$(S_{11}+S_{12})C_{133}+S_{13}C_{333}$
8*A*	[001]	[100]	[100]	$M_1\alpha T'$	S_{11}	$S_{11}C_{155}+S_{12}C_{144}+S_{13}C_{344}-2S_{14}C_{444}$
8*B*	[001]	[100]	[010]	$M_2\alpha T'$	S_{12}	$S_{12}C_{155}+S_{11}C_{144}+S_{13}C_{344}+2S_{14}C_{444}$
9*A*	[001]	[010]	[100]	$M_1\alpha T''$	S_{12}	$S_{11}C_{144}+S_{12}C_{155}+S_{13}C_{344}+2S_{14}C_{444}$
9*B*	[001]	[010]	[010]	$M_2\alpha T''$	S_{11}	$S_{12}C_{144}+S_{11}C_{155}+S_{13}C_{344}-2S_{14}C_{444}$
10*A*	$\left[0\frac{1}{\sqrt{2}}\frac{1}{\sqrt{2}}\right]$	$[0\ \alpha_3\ \beta_3]$	[100]		$\alpha_3^2S_{12}+\beta_3^2S_{13}+\alpha_3\beta_3S_{14}$	$\frac{1}{4}S_{11}(C_{111}+C_{112}+C_{114}+C_{123})$ $+\frac{1}{4}C_{222}(-S_{11}+S_{12})+C_{124}(S_{11}-2S_{12}-S_{14})$ $+C_{134}(S_{11}-S_{12}-S_{13}-S_{14})$ $+\frac{1}{4}C_{133}(S_{11}+S_{12}+2S_{13})$ $-\frac{1}{2}C_{114}(2S_{12}+S_{14})+C_{155}(S_{12}+2S_{14})$ $+\frac{1}{4}C_{113}(2S_{12}+S_{13})+C_{344}(S_{13}+2S_{14})$ $+S_{13}C_{333}+2S_{14}C_{444}$

TABLE VII. (*Continued*).

Mode	Propagation direction	Polarization direction	Stress direction	Case	F_U	G_U
10*B*	$\left[0\frac{1}{\sqrt{2}}\frac{1}{\sqrt{2}}\right]$	$[0\ \alpha_3\ \beta_3]$	$\left[0\ -\frac{1}{\sqrt{2}}\ \frac{1}{\sqrt{2}}\right]$		$\frac{1}{2}[S_{13}+\alpha_3^2(S_{11}+S_{14})$ $+\beta_3^2 S_{33}-\alpha_3\beta_3(S_{44}+S_{14})]$	$\frac{1}{8}(C_{111}+C_{112}+2C_{123})(S_{12}-S_{13}-2S_{14})$ $+\frac{1}{8}C_{222}(S_{11}-S_{12}+4S_{14})+\frac{1}{2}C_{114}(-S_{11}-2S_{14}+S_{44})$ $+\frac{1}{2}C_{124}(-2S_{11}+S_{12}-2S_{13}-6S_{14}+2S_{44})$ $+\frac{1}{2}C_{155}(S_{11}+S_{13}-2S_{44})$ $+\frac{1}{8}C_{113}(2S_{11}+2S_{13}+4S_{14}+S_{33})$ $+\frac{1}{2}C_{134}(-S_{11}+S_{12}-S_{13}-4S_{14}+2S_{44}-S_{33})$ $+\frac{1}{8}C_{133}(S_{11}+S_{12}+8S_{13}+2S_{33})$ $+\frac{1}{2}C_{344}(S_{13}-2S_{14}-4S_{44}+S_{33})$ $+\frac{1}{8}C_{333}(S_{13}+S_{33})$ $+\frac{1}{2}C_{144}(S_{13}-2S_{44})-C_{444}(S_{14}+2S_{44})$
11*A*	$\left[0-\frac{1}{\sqrt{2}}\frac{1}{\sqrt{2}}\right]$	$[0\ \beta_3\ -\alpha_3]$	[100]		$\beta_3^2 S_{12}+\alpha_3^2 S_{13}-\alpha_3\beta_3 S_{14}$	$\frac{1}{4}S_{11}(C_{111}+C_{112})+\frac{1}{4}C_{222}(S_{12}-S_{11})$ $-\frac{1}{4}S_{11}C_{123}+\frac{1}{4}C_{133}(S_{11}+S_{12}-2S_{13})$ $+\frac{1}{4}C_{113}(-2_{12}+S_{13})+\frac{1}{4}S_{13}C_{333}$ $+\frac{1}{2}S_{14}(-C_{114}-2C_{124}+4C_{444}+2C_{134})$
11*B*	$\left[0\frac{1}{\sqrt{2}}\frac{1}{\sqrt{2}}\right]$	$[0\ \beta_3\ -\alpha_3]$	$\left[0-\frac{1}{\sqrt{2}}\frac{1}{\sqrt{2}}\right]$		$\frac{1}{2}[S_{13}+\beta_3^2(S_{11}+S_{14})$ $+\alpha_3^2 S_{33}+\alpha_3\beta_3(S_{44}+S_{14})]$	$\frac{1}{8}[C_{111}(S_{12}+S_{13}-2S_{14})+C_{222}(S_{11}-S_{12})$ $+C_{112}(S_{12}+S_{13}-2S_{14})+C_{113}(-2S_{11}-4S_{14}+S_{33})$ $+C_{133}(S_{11}+S_{12}-S_{14})+C_{123}(-2S_{12}-S_{13}+4S_{14})$ $+C_{333}(S_{13}+S_{33})+C_{114}(2S_{14}+4S_{44})$ $+C_{124}(4S_{14}+4S_{44})+C_{134}(-4S_{14}-8S_{44})$ $+3S_{44}C_{155}]$
12*A*	$\left[0\frac{1}{\sqrt{2}}\frac{1}{\sqrt{2}}\right]$	[100]	[100]		S_{11}	$\frac{1}{4}C_{111}(-S_{11}+S_{12})-\frac{1}{8}C_{112}(S_{11}+S_{12})$ $+\frac{1}{8}C_{222}(3S_{11}-S_{12})+\frac{1}{2}C_{114}(S_{11}+S_{12})$ $+\frac{1}{2}C_{124}(3S_{11}-S_{12}+2S_{14})+\frac{1}{2}C_{155}(S_{11}+2S_{14})$ $+\frac{1}{2}C_{144}(S_{12}-2S_{14})+\frac{1}{2}S_{13}[\frac{1}{2}(C_{113}-C_{123})$ $+2C_{134}+C_{344}]$ $-2S_{14}C_{444}$

TABLE VII. (*Continued*).

Mode	Propagation direction	Polarization direction	Stress direction	Case	F_U	G_U
12*B*	$\begin{bmatrix} 0 \\ \frac{1}{\sqrt{2}} \\ \frac{1}{\sqrt{2}} \end{bmatrix}$	[100]	$\begin{bmatrix} 0 \\ -\frac{1}{\sqrt{2}} \\ \frac{1}{\sqrt{2}} \end{bmatrix}$	$\frac{1}{2}(S_{12}+S_{13}-S_{14})$		$\frac{1}{16}C_{111}(S_{11}+S_{12}+4S_{14})$
						$-\frac{1}{32}C_{112}(S_{11}+S_{12}+2S_{13})$
						$+\frac{1}{8}C_{222}(-\frac{1}{4}S_{11}+\frac{11}{4}S_{13}+3S_{12}-\frac{5}{2}S_{14})$
						$+\frac{1}{8}C_{114}(S_{11}+S_{12}+2S_{13})$
						$+\frac{1}{8}C_{124}(-S_{11}+2S_{13}+3S_{12}-10S_{14}-4S_{44})$
						$+\frac{1}{8}C_{144}(S_{11}+S_{13}+4S_{14}+S_{44})$
						$+\frac{1}{8}C_{155}(S_{12}+S_{13}-4S_{14}-4S_{44})$
						$+\frac{1}{8}[\frac{1}{2}(C_{113}-C_{123})+(2C_{134}+C_{344})(S_{13}+S_{33})$ $+\frac{1}{4}C_{444}(S_{14}+2S_{44})]$

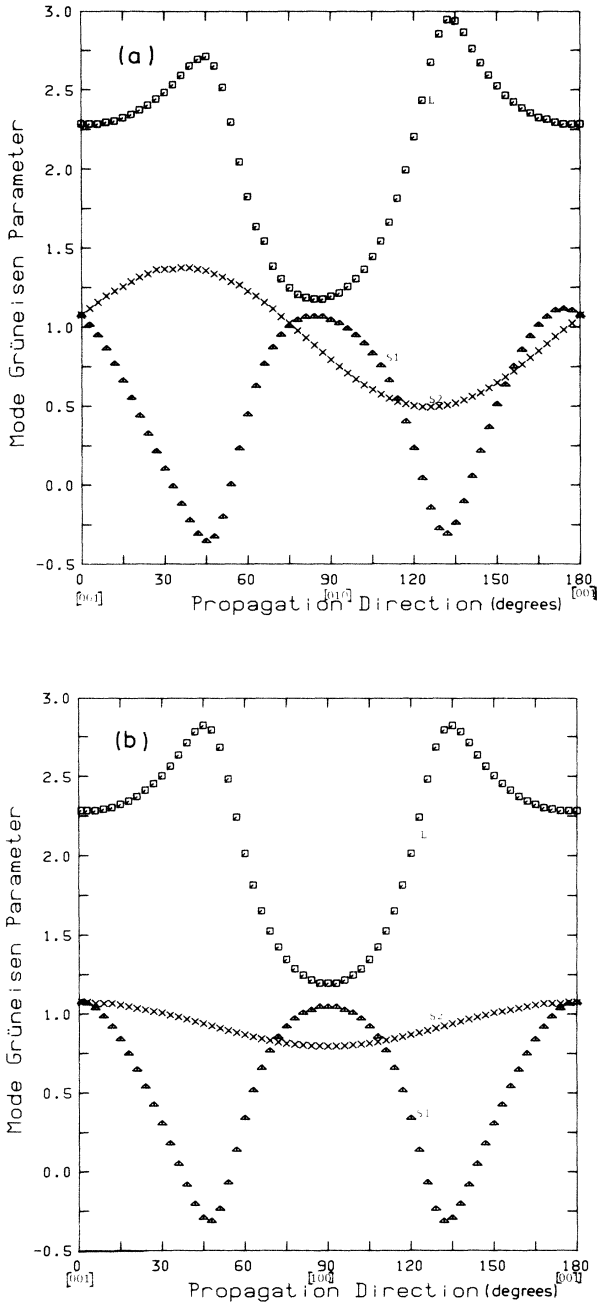

FIG. 5. The zone center acoustic-mode Grüneisen parameters as a function of propagation direction in (a) the *YZ* and (b) the *XZ* planes of $Pb_{4.7}Ba_{0.3}Ge_3O_{11}$.

For $Pb_5Ge_3O_{11}$ the Debye temperature [$=230$ K (Ref. 19)] is low enough to allow room temperature to be taken as the high-temperature limit, when the heat capacity per mode becomes Boltzmann's constant k. Then the mean Grüneisen parameter γ_H^{Br} takes the form of $(1/3N)\sum_{q,p}\gamma^{\mathrm{Br}}$. Here the superscript Br refers to the tensorial gamma defined by Brugger and Fritz[20] and discussed in Appendix A of Ref. 21. This summation has been carried out over a large number of acoustic modes to obtain high-temperature limits $(\gamma_{\|}^{\mathrm{Br}})_H$ and $(\gamma_{\perp}^{\mathrm{Br}})_H$ for

$Pb_5Ge_3O_{11}$ of $+1.68$ and 0.80, respectively, at 291 K. Hence the mean zone center acoustic-mode Grüneisen parameter is $+1.09$ in the high-temperature limit. Comparison of this value with 0.86 for γ^{th} indicates that the acoustic phonons deeper into the zone and the optic phonons together have a mean Grüneisen gamma rather less than unity: the soft ferroelectric mode can only have a slight influence on γ^{th} at room temperature.

ACKNOWLEDGMENTS

We are grateful to Dr. G. R. Jones (Royal Signals and Radar Establishment, Malvern, England) who provided the single crystals of $Pb_5Ge_3O_{11}$ and $Pb_{4.7}Ba_{0.3}Ge_3O_{11}$, to Mrs. W. A. Lambson for technical assistance in sample preparation, and to Dr. Y. K. Yoğurtcu for many useful discussions.

[1]H. Iwasaki, K. Sugii, T. Yamada, and N. Niizeki, Appl. Phys. Lett. **18** 444 (1971).
[2]H. Iwasaki, S. Miyazawa, H. Koizumi, K. Sugii, and N. Niizeki, J. Appl. Phys. **43**, 4907 (1972).
[3]T. Yamada, H. Iwasaki, and N. Niizeki, J. Appl. Phys. **43**, 771 (1972).
[4]G. R. Barsch, L. G. Bonczar, and R. E. Newnham, Phys. Stat. Sol. A **29**, 241 (1975).
[5]M. R. Houlton, G. R. Jones, and D. S. Robertson, J. Phys. D **8**, 219 (1975).
[6]A. G. Khatkevich, Kristallografiya **6**, 700 (1961) [Sov. Phys.—Crystallogr. **6**, 561 (1962)].
[7]F. I. Federov, *Theory of Elastic Waves in Crystals* (Plenum, New York, 1968).
[8]J. M. Farley and G. A. Saunders, J. Phys. C **5**, 3021 (1972).
[9]Y. K. Yoğurtcu, E. F. Lambson, A. J. Miller, and G. A. Saunders, Ultrasonics (1980). p. 155.
[10]R. N. Thurston and K. Brugger, Phys. Rev. **133**, A1604 (1964).
[11]Tu Hailing and G. A. Saunders, Philos. Mag. **48**, 571 (1983).
[12]H. J. McSkimin, P. Andreatch, and R. N. Thurston, J. Appl. Phys. **36**, 1624 (1965).
[13]H. Kaga, Phys. Rev. **172**, 900 (1968).
[14]R. E. Hankey and D. E. Schuele, J. Acoust. Soc. Am. **48**, 190 (1970).
[15]G. Burns and B. A. Scott, Phys. Lett. **39A**, 177 (1972).
[16]J. F. Ryan and K. Hisano, J. Phys. C **6**, 566 (1973).
[17]R. N. Thurston, H. J. McSkimin, and P. J. R. Andreatch, J. Appl. Phys. **37**, 267 (1966).
[18]Y. Nokagawa, K. Yamanouchi, and K. Shibayama, J. Appl. Phys. **44**, 3969 (1973).
[19]T. Suski and W. Muller-Lierheim, Phys. Stat. Sol. B **95**, 349 (1979).
[20]K. Brugger and T. C. Fritz, Phys. Rev. **157**, 524 (1967).
[21]T. H. K. Barron, J. G. Collins, and G. K. White, Adv. Phys. **29**, 609 (1980).